

Direct evidence for interface-induced perpendicular spin orientation and spin reorientation in terbium-coated thin iron films

B. Scholz, R. A. Brand, and W. Keune

Laboratorium für Angewandte Physik, Universität Duisburg, 47048 Duisburg, Germany

(Received 22 December 1993; revised manuscript received 25 April 1994)

Conversion-electron Mössbauer spectroscopy in ultrahigh vacuum has been employed to study *in situ* the average Fe-spin orientation and hyperfine fields in zero external field in uncoated and Tb-coated ^{57}Fe films deposited either onto a clean Tb(0001) single-crystal surface or onto (bulklike) polycrystalline Tb or Ag films. At 30 K, the spectra of 15-Å-thick uncoated Fe films on Tb(0001) indicate structurally disordered (amorphous) Fe layers, whereas spectra of 30- or 35-Å-thick uncoated and coated Fe films are typical for bcc Fe. We show that the orientation of Fe spins in 30–35-Å-thick uncoated Fe films is preferentially in the film plane for temperatures ranging from 30–300 K for all substrates used. In striking contrast to uncoated films Tb-coated 30–35-Å-thick Fe films exhibit a preferential Fe-spin orientation perpendicular to the film plane at ~ 30 K irrespective of the substrates used. This demonstrates (i) that the perpendicular spin orientation in these films originates from an interface magnetic anisotropy and (ii) that the dominant effect in inducing perpendicular spin direction originates from the interface formed by the Tb-coating layer and the Fe film and to a smaller extent to the Fe/Tb-substrate interface. A temperature-dependent reversible Fe-spin reorientation was observed near 150–200 K which is qualitatively compatible with recent models including spin fluctuations.

I. INTRODUCTION

The existence of a uniaxial perpendicular magnetic anisotropy (PMA) in certain homogeneous amorphous rare-earth-transition-metal (R - M) thin-film alloys for which the preferred direction of magnetization in zero external field is oriented perpendicular to the film plane was discovered by Chaudhari, Cuomo, and Gambino in 1973.¹ Since then, detailed studies of the magnetic properties of R - M alloy films have led to technological application of these materials as magneto-optical recording media.² In recent years, R - M multilayers have attracted considerable attention for reasons of basic interest and because of their potential for magneto-optical recording.^{3–6} The fundamental questions concern the origin of PMA and the magnetic coupling between neighboring R - M layers in multilayers. Sato⁶ reported that compositionally modulated Tb/Fe multilayers have large PMA for small individual layer thicknesses, and suggested that PMA is caused by an anisotropic spatial distribution of Tb-Fe pairs aligned preferentially perpendicular to the film plane. Since then, the magnetic properties of Tb/Fe multilayers have been investigated extensively.^{7–32} Antiferromagnetic (AF) coupling of Tb and Fe magnetic moments at the interface has also been established,^{8,12} similar to AF interactions in amorphous alloys. Shan and co-workers^{11–13} developed a model for the magnetic properties of R - M compositionally modulated films (CMF's) or multilayers ($R = \text{Dy, Tb}; M = \text{Co, Fe}$) in terms of the single-ion anisotropy of R ions with orbital momentum and an anisotropic distribution of R - M pairs oriented predominantly along the film-normal direction. This model focused on sputtered amorphous CMF structures with small individual layer thicknesses ($t_{\text{Tb}} = 4.5 \text{ \AA}$;

$t_{\text{Fe}} \leq 8.75 \text{ \AA}$), where severe intermixing of R and M atoms and amorphous alloy formation occurs across the interface and essentially through the entire multilayer.^{11–13} This model has been extended^{30–32} in order to describe PMA and other magnetic properties of Tb/Fe multilayers with larger individual layer thicknesses ($t_{\text{Tb}} \lesssim 26 \text{ \AA}$; $t_{\text{Fe}} \lesssim 40 \text{ \AA}$) where a substantial fraction of pure crystalline bcc Fe exists in the interior of individual Fe layers, in addition to a thin ($\sim 7 \text{ \AA}$) amorphous interface region.^{26–29}

The role of the interface is essential to understand PMA in these R - M multilayers. Mössbauer spectroscopy is a suitable method to separate the amorphous Fe state from the "bulklike" bcc Fe in Tb/Fe multilayers^{17,18,25–29} and other R - M multilayers.³³ It has been demonstrated by Mössbauer spectroscopy and electrical resistivity measurements^{17,18} that there is a correlation between the Tb-Fe alloy at the interface and PMA in such multilayers: a broader alloyed interface was claimed to orient the Fe-magnetic moments on the average more perpendicular to the film plane.^{17,18} In striking contrast, Mössbauer spectroscopy on Nd/Fe multilayers revealed an increase in the average perpendicular Fe-spin orientation by *decreasing* the amorphous interface fraction.¹⁹ Moreover, ^{57}Fe -Mössbauer spectroscopy may provide direct (microscopic) information about the average Fe-spin orientation (spin texture) in zero external field in a sample by comparing relative line intensities of a magnetically split sextet. The polar angle Θ between the incident γ -ray direction (being equal to the film-normal direction) and the direction of the magnetic hyperfine field B_{hf} or Fe-spin direction, is obtained from the line-intensity ratios 3: x :1:1: x :3 of the six Mössbauer lines, where x is related to Θ by $\cos^2\Theta = (4-x)/(4+x)$. The

measured values of $\cos^2\Theta$ are spatial averages of $\langle \cos^2\Theta \rangle$ over the sample. Usually, an average "cone angle" (or tilt angle) $\langle \Theta \rangle$ is defined by $\arccos(\langle \cos^2\Theta \rangle)^{1/2}$, Fig. 1. Complete perpendicular spin orientation is indicated by ratios 3:0:1:1:0:3 or $\langle \Theta \rangle = 0^\circ$, whereas complete in-plane orientation is present for ratios 3:4:1:1:4:3 or $\langle \Theta \rangle = 90^\circ$. A random Fe-spin texture is equivalent to the ratio 3:2:1:1:2:3 or $\langle \Theta \rangle = 54.7^\circ$. Several Mössbauer-effect studies have demonstrated strong but incomplete perpendicular spin texture in certain Tb/Fe multilayers, with the smallest $\langle \Theta \rangle$ values reported ranging from 11° (Ref. 15) to 20° – 32° .^{18,25,27,28}

Up to now, the vast majority of studies of the Tb/Fe system have used multilayers which by their nature contain a large number (of the order of several tens or hundreds) of stacked Tb/Fe bilayers, or equivalently, a large number of Tb/Fe interfaces.^{6–29} However, the elementary building block of a multilayer, namely the *R*/Fe bilayer, has scarcely been investigated. Rau and Xing³⁴ studied uncoated and Tb-coated Fe(001) films on an Ag(001) substrate by electron-capture spectroscopy. They report large temperature-dependent out-of-plane magnetic texture at surfaces of Tb-coated Fe(001) films 1–10 monolayers (ML) thick on Ag(001), in striking contrast to uncoated Fe(001)/Ag(001) films which exhibit in-plane magnetic texture. Furthermore, monolayer coverages of *R* metals (Gd, Tb, Dy, and Nd) on the Fe(001) single-crystal surface have been investigated with spin-resolved photoelectron spectroscopy by Carbone *et al.*,³⁵ providing direct evidence of antiferromagnetic coupling between the heavy *R* and (in-plane) Fe-spin moments, and of ferromagnetic coupling between Nd and (in-plane) Fe magnetic moments, at the *R*/Fe interface. In another study of *R*-Fe interaction, layer-dependent spin-resolved photoemission results by Vescovo *et al.*³⁶ revealed that Sm overlayers at the Fe(001) surface are magnetically ordered with a ferromagnetic spin component in the interface plane, and with antiferromagnetic coupling of the in-plane Sm and Fe moments.

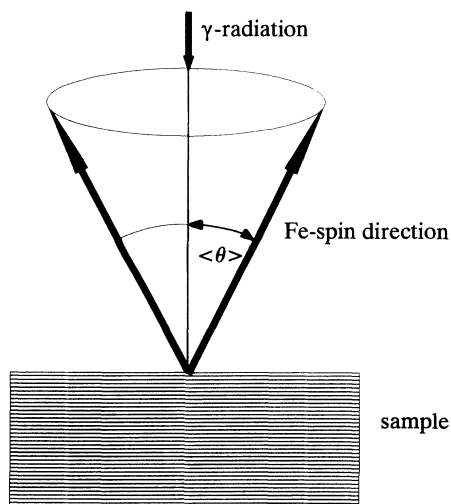


FIG. 1. Geometrical relationship between γ -ray direction, sample plane, Fe-spin direction, and average cone angle $\langle \Theta \rangle$.

In this paper we present experimental results describing the influence of the Tb/Fe interface on the preferential Fe-spin orientation and its temperature dependence in a single layer of Fe. The main aim of this work was to provide a microscopic characterization of the magnetic structure in zero external field in an Fe film interfaced by Tb. ^{57}Fe conversion-electron Mössbauer spectroscopy (CEMS) is well suited to study thin-film phenomena *in situ* under ultrahigh-vacuum conditions.^{37–39} We will show that a single Fe/Tb interface is not sufficient to induce strong perpendicular spin texture in a bcc-Fe film, and that the dominant effect originates from the Tb-coating layer producing a Tb/Fe interface.

II. SAMPLES AND EXPERIMENTS

All experiments were performed *in situ* in an ultrahigh-vacuum (UHV) system with a base pressure $p \leq 2 \times 10^{-10}$ mbar. ^{57}Fe layers were grown by thermal evaporation onto three different types of substrates: (i) an oriented Tb(0001) single-crystal surface, (ii) a polycrystalline (150 Å) Tb thin-film surface, and (for comparison) (iii) a polycrystalline (300 Å) Ag thin-film surface.

(i) The Tb(0001) substrate was obtained from an (0001)-oriented Tb single crystal (~ 10 mm in diameter, ~ 2 mm thick) which first was mechanically polished using alumina suspensions down to a grain size of $0.05 \mu\text{m}$. Subsequently, the Tb single-crystal surface was cleaned in UHV by repeated cycles of Ar-ion sputtering (4–5 keV) and annealing at temperatures ≤ 673 K. The first (weak) diffraction spots in RHEED (reflection high-energy electron diffraction) appeared on the average after a total of 44 h of sputtering and annealing at an ion energy of 4.4 keV and annealing at 600 K. After further sputtering and annealing at 4 keV and 673 K for 20 h, clear LEED (low-energy electron diffraction) and RHEED patterns could be observed. No surface contaminants except a small amount of oxygen could be detected by Auger electron spectroscopy (AES). The smoothness and cleanliness of this Tb surface was further improved by deposition of a 200-Å-thick homoepitaxial Tb(0001) layer grown at 673 K at a rate of 0.1 \AA/s . This treatment resulted in little oxygen contamination of the Tb(0001) surface as revealed by AES [Fig. 2(a)], and in clear LEED and RHEED patterns (with RHEED spots lying on circles) indicating a well-ordered structure and a nearly atomically flat surface (Fig. 3).

^{57}Fe films of 3, 15, and 30 Å in thickness were deposited onto such clean Tb(0001) surfaces at 295 K at a rate of 0.01 \AA/s for the 3-Å film and 0.05 \AA/s for the 15- and 30-Å films. By AES, these films were found to be free from contamination [Fig. 2(b)]. Since no LEED or RHEED spots could be observed on these Fe films, they were polycrystalline or structurally disordered. Special attention was paid to the Fe(30 Å)/Tb(0001) film: after CEMS measurements on this uncoated sample, it was covered with a polycrystalline top layer of 14-Å Tb, and subsequently CEMS experiments were repeated with this coated Tb(14 Å)/Fe(30 Å)/Tb(0001) specimen. In this case, it was revealed by lateral-scanning AES that only 70% of this Fe-film area was covered by the 14-Å Tb lay-

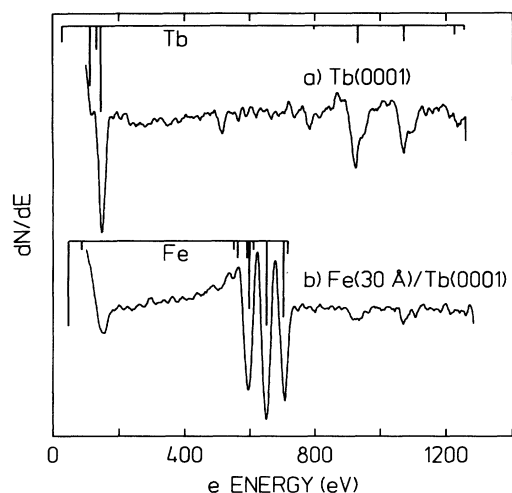
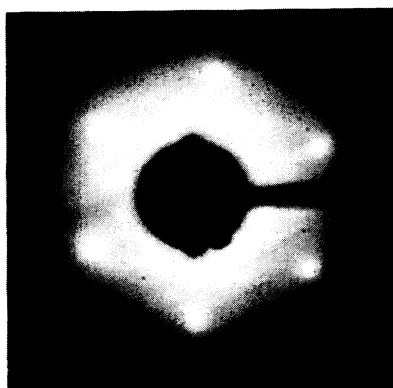


FIG. 2. (a) Auger-electron spectrum of the clean Tb(0001) surface [clean Tb(0001) single-crystal surface coated by a 200-Å-thick homoepitaxial Tb(0001) layer] prior to ⁵⁷Fe-film deposition. (b) Auger-electron spectrum of a 30-Å-thick ⁵⁷Fe film directly after deposition. The drawn bar diagrams indicate the position of the Tb and Fe lines, respectively.



(a)



(b)

FIG. 3. (a) $p(1 \times 1)$ LEED pattern (electron energy 45 eV) and (b) RHEED pattern (electron energy 9 keV) of the clean Tb(0001) surface prior to ⁵⁷Fe-film deposition.

er due to experimental difficulties. This observation had to be considered in the evaluation of Mössbauer data from this only partially coated sample (see Sec. III B).

(ii) The polycrystalline Tb surface was obtained by deposition of a 150-Å-thick polycrystalline Tb layer onto a Cu(001) single-crystal surface. The Cu(001) crystal was chosen since it provides a clean and atomically flat surface after repeated cycles of Ar sputtering and annealing. This has been demonstrated by the observation of sharp LEED spots and streaks in the RHEED pattern.⁴⁰ The 150-Å Tb layer was grown at 295 K with a rate of 0.1 Å/s. Subsequently, a 35-Å-thick polycrystalline ⁵⁷Fe film was grown on the Tb layer at 295 K, resulting in the Fe(35 Å)/Tb(150 Å)/Cu(001) sample. Both the Tb and Fe films were polycrystalline, as revealed by the absence of LEED and RHEED spots. After CEMS measurements on this uncoated specimen, the Fe film was completely covered by a top layer of 14-Å Tb, and subsequently CEMS experiments were performed on this coated Tb(14 Å)/Fe(35 Å)/Tb(150 Å)/Cu(001) sample.

(iii) For comparison, a polycrystalline 35-Å-thick ⁵⁷Fe layer was deposited at 295 K onto the surface of a polycrystalline 300-Å-thick Ag film which had been grown at 295 K at a rate of 0.5 Å/s on a polycrystalline Al substrate. This substrate had been flattened by mechanical polishing. CEMS experiments were performed on an uncoated Fe(35 Å)/Ag(300 Å)/Al sample, and subsequently on the same specimen after complete coating by 14-Å Tb.

The nomenclature and description of the samples prepared for this study are summarized in Table I.

The materials ⁵⁷Fe metal (95% enriched in ⁵⁷Fe), Tb of purity 99.99 at. %, and Ag of purity 99.999 at. %, were thermally evaporated from alumina crucibles (for ⁵⁷Fe and Ag) or from a W crucible (for Tb) in resistively heated Knudsen-cell-type ovens built in our laboratory. Each oven was surrounded by Mo heat shields and a water-cooled shroud. The distance between the oven openings and the substrate was about 40 cm. The pressure during evaporation was $\lesssim 3 \times 10^{-9}$ mbar for ⁵⁷Fe, $\lesssim 4 \times 10^{-9}$ mbar for Tb, and $\lesssim 2 \times 10^{-9}$ mbar for Ag. The deposition rate and film thickness were monitored by a calibrated quartz microbalance located close to the substrate position. The sample temperature could be varied in the range between 30 and 700 K with an accuracy of ~ 5 K by using either a liquid-helium flow cryostat (integrated into the UHV sample manipulator) or a resistively heated substrate holder.

TABLE I. Sample composition and assignments.

Sample	Composition
A	Fe(30 Å)/Tb(0001)
B	Tb(14 Å)/Fe(30 Å)/Tb(0001) (Fe surface only 70 % coated by top Tb layer)
C	Fe(35 Å)/polycr. Tb(150 Å)/Cu(001)
D	Tb(14 Å)/Fe(35 Å)/polycr. Tb(150 Å)/Cu(001)
E	Fe(35 Å)/Ag(300 Å)/Al
F	Tb(14 Å)/Fe(35 Å)/Ag(300 Å)/Al
G	Fe(3 Å)/Tb(0001)
H	Fe(15 Å)/Tb(0001)

Conversion electrons were detected *in situ* by use of a spherical electrostatic electron-energy analyzer of 2% energy resolution⁴¹ and a modified channeltron detector.⁴² The experimental setup will be described in detail elsewhere.⁴¹ The electron-energy analyzer served as a filter for 7.3-keV *K*-conversion electrons in order to suppress the high photoelectron background from the Tb layer, and to improve the signal-to-noise ratio. The 14.4-keV γ radiation from a ⁵⁷Co(Rh) source of about 50–100-mCi activity was set in normal incidence to the film plane by turning the sample into the appropriate position via the UHV manipulator. The typical measuring time for obtaining a useful Mössbauer spectrum was about 1–13 days, depending on the thickness of the ⁵⁷Fe layer.

III. RESULTS

A. Uncoated Fe on Tb(0001)

1. Fe thickness ≤ 15 Å

Typical Mössbauer spectra of uncoated ⁵⁷Fe films of various thicknesses on Tb(0001) measured at 295 or 30 K are shown in Fig. 4.

The spectrum taken at 295 K from sample *G*, i.e., from

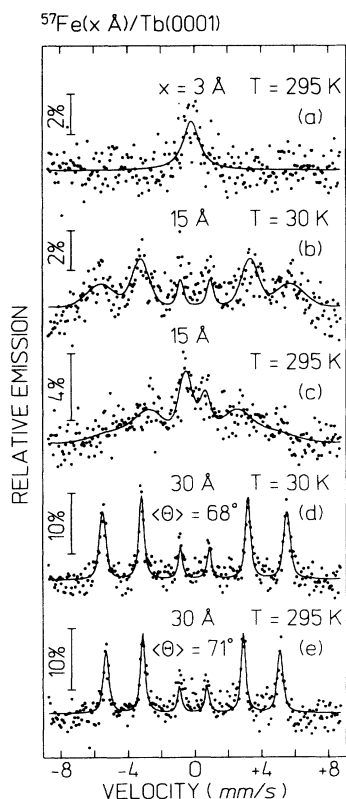


FIG. 4. CEM spectra of uncoated ⁵⁷Fe films of various thicknesses deposited onto Tb(0001) and measured at different temperatures *T*: (a) sample *G*, *T* = 295 K; (b) sample *H*, *T* = 30 K; (c) sample *H*, *T* = 295 K; (d) sample *A*, *T* = 30 K; and (e) sample *A*, *T* = 295 K. The average cone angle $\langle \Theta \rangle$ is indicated in (d) and (e). (The full drawn curves are least-squares fits described in the text).

3-Å Fe on Tb(0001), or slightly more than about two monolayers (ML) of Fe on Tb(0001), exhibits only a central feature [Fig. 4(a)] which indicates paramagnetism at room temperature. This spectrum interpreted as a broad single Lorentzian line shows a linewidth [full width at half maximum (FWHM)] of ~ 1.2 mm/s which is much larger than the measured linewidth in a standard bcc-Fe calibration spectrum (0.23 mm/s) measured in this system. This large linewidth is very likely due to an unresolved quadrupole splitting which results from interactions of the ⁵⁷Fe atoms with their surrounding Tb-neighbor atoms. The quadrupole splitting $\Delta E_Q = |eQV_{zz}/2|\sqrt{1-\eta^2}/3$ estimated from the linewidth is about 0.6 mm/s, in fair agreement with the value of 0.46 mm/s reported for Fe(3 Å)/Tb multilayers.²⁵ The central line shift (isomer shift) δ was 0.06(4) mm/s with respect to bcc Fe at 300 K. It is not known at present if this spectrum indicates that the ordering temperature of the film is below room temperature, or if it is superparamagnetic.

The spectra of thicker Fe films on Tb(0001) show magnetic-hyperfine splitting at 295 and 30 K [Fig. 4(b)–(e)]. The magnetically split sextet of sample *H*, i.e., 15-Å Fe on Tb(0001), at 30 K is characterized by very broad lines [Fig. 4(b)], indicating a distribution of hyperfine fields $P(B_{hf})$. This is typical for a crystallographically disordered structure, such as amorphous iron, and is observed, for instance, in amorphous Fe-Y (Ref. 43) bulk alloys, amorphous Fe-Tb thin-film alloys,⁴⁴ and at the interface in Tb/Fe multilayers^{17,18,25–29} and other *R*/Fe multilayers.³³ The spectrum in Fig. 4(b) was evaluated using a Gaussian hyperfine distribution $P(B_{hf})$ (resulting in Voigt profile lines). From such an analysis of the spectra in Figs. 4(b) and 4(c), values of 35.1 T at 30 K and 27.8 T at 295 K have been obtained for the average hyperfine field B_{hf} and a standard deviation σ of the hyperfine-field distribution of 4.8 T at 30 K and 8.0 T at 295 K. Moreover, from the relative line intensities the averaging cone angle $\langle \Theta \rangle$ was found to be 70° – 90° at 30 and 295 K, indicating a strong tendency for in-plane magnetic anisotropy for Fe(15 Å)/Tb(0001) at these temperatures. The hyperfine-field value of 35.1 T at 30 K for this uncoated amorphous 15-Å film is clearly larger than that of bulk bcc Fe at 30 K (34 T), and is also larger than that observed in amorphous Y-Fe bulk alloys,⁴³ Tb-Fe thin-film alloys,⁴⁴ and at the interface of Tb/Fe multilayers^{17,18,25–28} and other *R*/Fe multilayers.^{33,45} For instance, the saturation hyperfine field of coated 15-Å-thick amorphous Fe layers in Y(30 Å)/Fe(15 Å)/Y(70 Å) triple layers was measured to be only 25.0 T,⁴⁵ which is much less than our value of 35.1 T for uncoated amorphous Fe(15 Å)/Tb(0001). A possible reason for this different behavior could be a lower mass density of the uncoated amorphous Fe layer in Fe(15 Å)/Tb(0001) as compared to the density of amorphous Fe in trilayers or multilayers, since the Fe magnetic moment was calculated to increase with decreasing density in amorphous Fe,⁴⁶ and since the hyperfine field is usually approximately proportional to the Fe moment.⁴⁷

For fitting the 295-K spectrum in Fig. 4(c), a central quadrupole-split doublet (with $\Delta E_Q = 1.2$ mm/s) had to

be taken into account in addition to the broadened sextet. One can conclude from the relative spectral area of this doublet that a fraction of 36% of the Fe atoms in this amorphous 15-Å Fe film is paramagnetic at 295 K, equivalent to a film thickness of 5.4 Å or about two Fe monolayers. The asymmetry in the line intensities (area ratio 0.4 ± 0.1) of this doublet indicates the presence of a preferred direction of the main component V_{zz} of the electric-field gradient (EFG) tensor, i.e., a certain crystallographic or anisotropic short-range order, in this amorphous film.

Since a magnetic splitting is still present in the 295-K spectrum [Fig. 4(c)] of the amorphous 15-Å Fe layer on Tb(0001), its Curie temperature T_c must be above room temperature. This is in striking contrast to 15-Å-thick amorphous Fe films in Y/Fe/Y trilayers,⁴⁵ which exhibit a T_c of only about 70 K, implying a weaker exchange interaction than in amorphous Fe(15 Å)/Tb(0001). On the basis of mean-field theory, Honda, Kimura, and Nawate¹⁰ have calculated the Curie temperature in Tb/Fe multilayers and have shown that the rather high- T_c values of amorphous Fe (with an assumed fcc-like structure) in Tb/Fe multilayers result from an enhancement of the ex-

change interaction due to the Fe-Tb interaction at the interface. Since Y has no magnetic moment, such an enhancement is not expected in Y/Fe multilayers. Spectral Mössbauer parameters of this sample are listed in Table II.

2. Fe thickness 30 Å

The Mössbauer spectra of the uncoated 30-Å-thick Fe film on Tb(0001) (sample *A*) at 30 and 295 K show magnetically split sextets with relatively narrow lines typical for crystalline bcc Fe [Figs. 4(d) and 4(e)]. These spectra (as well as all other magnetically split spectra discussed in this paper) have been least squares fitted with sextets of Lorentzian lines using a Voigt profile for the line shapes, implying a Gaussian distribution of $P(B_{\text{hf}})$. This type of fitting has been employed since the linewidth was observed to be slightly larger than that of a bulk- α -Fe calibration foil [0.232(7) mm/s], indicating a narrow distribution of hyperfine fields, possibly as a result of inhomogeneous strain. The average hyperfine field B_{hf} obtained was 34.1 T at 30 K and 32.2 T at 295 K, in good agreement with corresponding values for bulk bcc Fe (34 and 33 T, respectively). Average cone angles of 68° at 30 K and 71° at 295 K have been obtained from the relative line intensities, implying preferential Fe-spin orientation in the film plane, similar to the case of the Fe(15 Å)/Tb(0001) sample. This in-plane spin orientation is not complete, however, since a complete in-plane spin texture would mean $\langle \Theta \rangle = 90^\circ$. Spectral Mössbauer parameters of sample *A* are summarized in Table II.

Our observation that uncoated 15- or 30-Å-thick Fe films on Tb(0001) exhibit preferential in-plane Fe-spin orientation at 30 and 295 K is quite different from results obtained from multilayered Tb/Fe samples with similar individual Fe-layer thicknesses. In our earlier work we have demonstrated by Mössbauer spectroscopy that Tb/Fe multilayers with an individual Fe-layer thickness t_{Fe} of 30 Å and below show a preferred perpendicular Fe-spin direction independent of temperature for individual Tb-layer thicknesses t_{Tb} of 7 and 14 Å, and an Fe-spin reorientation from the perpendicular direction (below ~ 100 K) to an in-plane easy direction (at 295 K) for $t_{\text{Tb}} = 26$ Å.²⁶⁻²⁹ Obviously, an uncoated single Fe layer on the surface of a bulk Tb single crystal behaves differently.

The drastic change in the appearance of the spectra in Figs. 4(b) and 4(c) as compared with those of Figs. 4(d) and 4(e) is the result of an irreversible retrocrystallization of the amorphous Fe (at $t_{\text{Fe}} = 15$ Å) to bcc Fe (at $t_{\text{Fe}} = 30$ Å) involving almost the whole layer thickness except for a thin remaining interface layer [which could not be detected in Figs. 4(d) and 4(e) due to the low signal-to-noise ratio]. This change has been reported earlier for Tb/Fe multilayers^{15-18,20,24-29} and for other R/Fe multilayered films.^{19,33,45,48} It has been detected indirectly by *in situ* resistance measurements during film growth.¹⁷

TABLE II. Spectral Mössbauer parameters obtained from the different samples. B_{hf} is the magnitude of the average hyperfine field, δ is the isomer shift (relative to α -Fe at 300 K), $\Delta E_Q = eV_{zz}Q/2$ is the quadrupole splitting, WID = FWHM (linewidth), σ is the Gaussian standard width of the hyperfine-field distribution, and $\langle \Theta \rangle$ the average cone angle.

Sample	T [K]	B_{hf} [T]	σ [T]	δ [mm/s]	$\langle \Theta \rangle$ [$^\circ$]
<i>A</i>	30	34.13(6)	0.8(1)	0.129(7)	68(5)
<i>A</i>	295	32.22(7)	0.6(1)	0.012(8)	71(5)
<i>B</i>	30	34.67(6)	1.11(9)	0.12(6)	32(5)
<i>B</i>	150	34.1(1)	0.9(1)	0.09(1)	27(5)
<i>B</i>	200	33.35(8)	1.0(1)	0.04(1)	49(5)
<i>B</i>	295	32.13(6)	0.90(9)	0.011(7)	63(5)
<i>C</i>	35	34.06(7)	0.8(1)	0.119(7)	74(5)
<i>D</i>	35	35.29(4)	0.78(5)	0.114(5)	28(5)
<i>D</i>	100	35.0(1)	1.0(1)	0.10(1)	28(5)
<i>D</i>	150	34.9(1)	0.8(1)	0.09(1)	31(5)
<i>D</i>	200	34.47(7)	0.6(1)	0.07(1)	31(5)
<i>D</i>	295	32.11(7)	0.7(1)	-0.002(4)	76(5)
<i>E</i>	40	34.38(3)	1.37(4)	0.171(3)	80(5)
<i>E</i>	295	31.70(5)	1.16(6)	0.035(5)	83(5)
<i>F</i>	40	34.71(3)	1.08(5)	0.155(4)	57(5)
<i>F</i>	100	34.25(4)	1.00(6)	0.135(5)	59(5)
<i>F</i>	200	32.87(6)	0.9(1)	0.097(8)	76(5)
<i>F</i>	295	31.77(4)	1.13(5)	0.039(4)	81(5)
<i>G</i>	295	Single Line:	δ : 0.05(4) mm/s; WID: 0.8(1) mm/s		
<i>H</i>	30	35.1(2)	4.8(4)	0.18(2)	70-90
<i>H</i>	295	27.8(1.1)	8.0(1.5)	0.03(8)	70-90
		Doublet:	ΔE_Q : 1.2(2) mm/s; δ : 0.26(9) mm/s; WID: 1.0 mm/s		

B. Tb-coated Fe on Tb(0001)

Typical Mössbauer spectra of the Tb-coated 30-Å Fe film on Tb(0001) (sample *B*) at different temperatures are displayed in Fig. 5. The spectra and their Mössbauer parameters (Table II) are typical for bcc Fe and similar to those of the uncoated film [Figs. 4(d) and 4(e)] except for very different spin texture (line-intensity ratios) at low temperatures. This striking difference can clearly be seen by comparing the spectra taken at 30 K and shown in Figs. 5(a) and 4(d). The relative intensity of the second and fifth Mössbauer lines has dramatically decreased in Fig. 5(a) as compared to Fig. 4(d), as a result of the Tb coating. This demonstrates that preferential out-of-plane Fe-spin orientation is induced by the Tb-coating layer in sample *B*, while preferential in-plane spin orientation was present in the uncoated film (sample *A*). Comparison of the relative line intensities in Figs. 5(a) and 5(b) reveals that out-of-plane spin orientation is still retained in sample *B* at 150 K. The corrected cone angle $\langle \Theta \rangle$ obtained for sample *B* at 30 K is only 32°, as compared to a corresponding value of 68° for sample *A*. At a certain temperature, the true (corrected) $\langle \Theta \rangle$ value of the fraction of the Fe film covered completely by Tb was calculated from the measured $\langle \Theta \rangle$ value by assuming that the uncovered 30% of the Fe film retains the $\langle \Theta \rangle$ value determined for sample *A* (uncoated) at that temperature. These corrected values of $\langle \Theta \rangle$ for sample *B* are listed in Table II, together with its other spectral parameters. At 295 K,

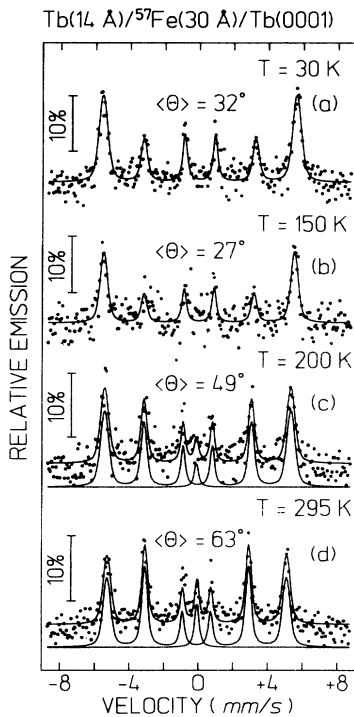


FIG. 5. CEM spectra of a 30-Å-thick ^{57}Fe film deposited onto Tb(0001) and coated by 14-Å Tb (sample *B*), measured at (a) $T=30$ K, (b) $T=150$ K, (c) $T=200$ K, and (d) $T=295$ K. The average cone angle is indicated in each case. (The full drawn curves are least-squares fits described in the text.)

$\langle \Theta \rangle$ of sample *B* is found to be 65°, implying incomplete in-plane Fe-spin orientation. Thus, with increasing T , the preferential Fe-spin direction in sample *B* in zero external field changes from perpendicular (at low T) to nearly in plane (at 295 K), as has already been found for Tb/Fe multilayers.^{18,20,27,28,32}

Analysis of the 295-K spectrum [Fig. 5(d)] of sample *B* (coated) indicated a central (paramagnetic) spectral component of $\sim 8\%$ in relative intensity in addition to the dominant sextet. By fitting this central component with a Lorentzian single line, a linewidth of only 0.28 mm/s and a central line shift (isomer shift δ) of $+0.039 \pm 0.020$ mm/s (relative to α -Fe at 295 K) was obtained. This rather sharp single line is barely detectable at 200 K [Fig. 5(c)], and has certainly disappeared at 30 K [Fig. 5(a)]. We cannot claim that such a single-line component was present also in the spectrum of sample *A* (uncoated) at 295 K, as the counting statistics was not good enough in this case [Fig. 4(e)]. The origin of this weak single-line component is not yet clear, although its central line-shift value δ (being close to zero) and its disappearance at low T suggests that it is due to a small fraction of superparamagnetic bcc-Fe clusters in the film. In addition it shows no quadrupole effect and so implies a cubic site.

C. Uncoated and Tb-coated Fe on polycrystalline Tb

It is interesting to check whether the single-crystalline nature of the Tb(0001) substrate is responsible for the Fe-spin orientational effects described in Secs. III A and III B. For this reason, the experiments described above have been repeated using a polycrystalline (bulklike) 150-Å-thick hcp-Tb layer as a substrate for the Fe film (35 Å thick in this case).

Mössbauer spectra of these specimens at different temperatures, i.e., of samples *C* (uncoated) and *D* (Tb coated), are shown in Fig. 6. All spectra are typical for bcc Fe. Parameters are summarized in Table II. The Fe-spin orientational phenomena observed with this polycrystalline Tb substrate are similar to those obtained with the Tb(0001) substrate. Thus the uncoated Fe film on polycrystalline Tb (sample *C*) at 35 K exhibits preferential in-plane orientation with an angle $\langle \Theta \rangle$ of 74° [Fig. 6(a)], in good agreement with the result obtained from sample *A* at 30 K [Fig. 4(d)]. On the other hand, clear out-of-plane Fe-spin texture is induced by the Tb-coating layer in sample *D* at temperatures ranging between 35 and 200 K, as is indicated by the relative line intensities in Figs. 6(b)–6(d). The cone angle $\langle \Theta \rangle$ obtained from the 35-K spectrum [Fig. 6(b)] is equal to 28°, in good agreement with the (corrected) value of 32° of sample *B* at 30 K. At 295 K, the Fe-spin texture of sample *D* has changed to incomplete in-plane orientation $\langle \Theta \rangle = 76^\circ$ [Fig. 6(e)], which is somewhat larger than the (corrected) value of $\langle \Theta \rangle = 63^\circ$ obtained for sample *B* at room temperature. Other parameters of samples *C* and *D* are given in Table II.

Figure 7 displays the temperature dependence of measured $\langle \Theta \rangle$ values for samples *A*–*D*. For the Tb-coated samples *B* and *D*, the Fe-spin reorientation from the preferred perpendicular direction at low temperatures to

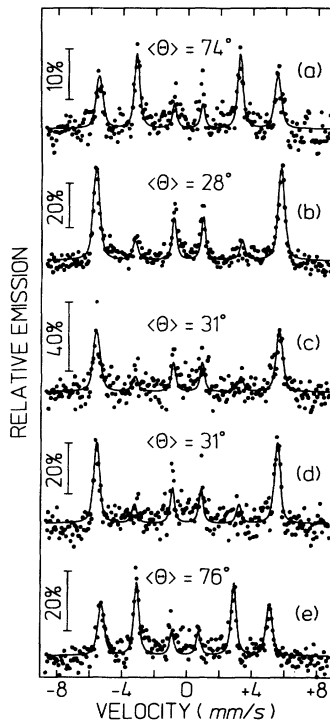


FIG. 6. CEM spectra of 35-Å-thick ^{57}Fe film deposited onto 150-Å polycrystalline Tb on Cu(001) substrate: (a) uncoated (sample *C*) measured at $T=35$ K; (b)–(e) coated by 14-Å Tb (sample *D*), measured at (b) $T=35$ K, (c) $T=150$ K, (d) $T=200$ K, and (e) $T=295$ K. The average cone angle $\langle \Theta \rangle$ is indicated in each case. (The full-drawn curves are least-squares fits described in the text.)

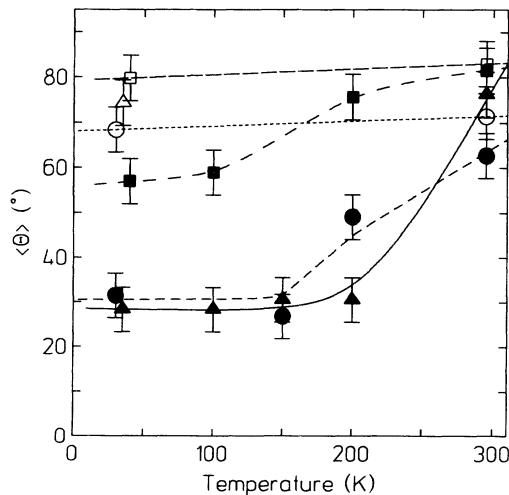


FIG. 7. Results for the average cone angle $\langle \Theta \rangle$ as a function of temperature for the different samples studied: sample *A*, open circles; sample *B*, full circles; sample *C*, open triangle; sample *D*, full triangles; sample *E*, open squares; and sample *F*, full squares. (The drawn curves serve as guides to the eyes.)

preferential in-plane orientation at higher temperature sets in at ~ 150 K for sample *B* [Tb(0001) substrate] and at ~ 200 K for sample *D* (polycrystalline Tb substrate). For sample *A* (uncoated), the change in $\langle \Theta \rangle$ with temperature can be seen to be small.

D. Uncoated and Tb-coated Fe on polycrystalline Ag

Results obtained so far emphasize the important role of the top-Tb layer in inducing the perpendicular anisotropy responsible for the out-of-plane magnetic texture. In order to eliminate the effect of the Tb substrate and concentrate on the influence of the Tb coating layer alone, samples *E* and *F* [both of which contain 35-Å ^{57}Fe on a polycrystalline (bulklike) Ag substrate] have been studied.

A polycrystalline Ag substrate has been chosen since essentially in-plane magnetic anisotropy may be expected for 35-Å Fe on this substrate in the whole temperature range studied due to the predominant shape anisotropy of this Fe film. Although a perpendicular anisotropy has been observed for ultrathin epitaxial bcc-Fe layers of 2.4–3 monolayers (~ 3.4 – 4 Å) in thickness on a Ag(001) substrate^{39,49} below 15 K, and for polycrystalline 5-Å-thick Fe films on polycrystalline Ag at 4.2 K,⁵⁰ thicker Fe films (≥ 9 ML or ~ 13 Å) on Ag(001) exhibit preferred in-plane anisotropy even at 4.2 K,⁴⁹ and the same is true for 5.5-ML Fe films on Ag(001) at 300 K.³⁹ For instance,

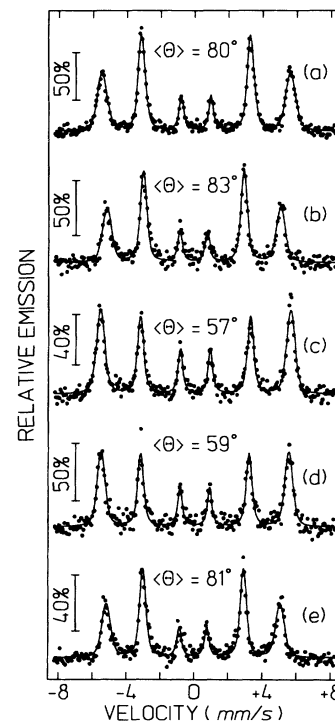


FIG. 8. CEM spectra of 35-Å-thick ^{57}Fe film deposited onto a 300-Å-thick polycrystalline Ag film on an Al substrate: uncoated (sample *E*), measured at (a) $T=40$ K and (b) $T=295$ K; (c)–(e) coated by 14-Å Tb (sample *F*), measured at (c) $T=40$ K, (d) $T=100$ K, and (e) $T=295$ K. The average cone angle $\langle \Theta \rangle$ is indicated in each case. (The full drawn curves are least-squares fits described in the text.)

$\langle \Theta \rangle = 73^\circ$ is found for 9-ML Fe on Ag(001) at 4.2 K.⁴⁹ Perpendicular anisotropy does not exist in ultrathin Fe(110) even in the monolayer range on Ag(111) at 4.2 K or higher temperatures.⁵¹ Therefore, for our rather thick (uncoated) polycrystalline 35-Å (~25-ML) Fe film on polycrystalline Ag, preferred in-plane Fe-spin orientation is to be expected for all temperatures used here.

This is confirmed by the spectra of sample *E* [Fe(35 Å)/Ag(300 Å)] at 40 and 295 K [Figs. 8(a) and 8(b)]. These spectra [as well as those of sample *F*, Figs. 8(c)–8(e)] are typical for bcc Fe. For the uncoated Fe(35 Å)/Ag(300 Å) film (sample *E*), cone angles $\langle \Theta \rangle$ of 80° and 83° at 40 and 295 K, respectively, have been obtained, which indicates strong preferred in-plane Fe-spin texture nearly independent of temperature, as expected. The striking effect of a 14-Å Tb coating layer covering this sample is revealed by the intensity ratio in the spectrum of sample *F* [Tb(14 Å)/Fe(35 Å)/Ag(300 Å)] at 40 K [Fig. 8(c)] from which a cone angle $\langle \Theta \rangle$ of 57° is obtained (Fig. 7). This means that the average Fe-spin direction has changed from nearly completely in plane ($\langle \Theta \rangle = 80^\circ$) for the uncoated film toward the out-of-plane direction for the Tb-coated film. On the other hand, at 295 K the average angle $\langle \Theta \rangle$ is found from Fig. 8(e) to be the same within error limits for samples *F* (82°) and *E* (83°) (Fig. 7), indicating nearly perfect in-plane Fe-spin texture.

The measured average hyperfine-field values as a function of temperature obtained for the different samples are displayed in Fig. 9.

From Table II we notice that the values for the isomer shift δ of samples *A*–*F* are identical within error limits to those of bulk bcc Fe. Moreover, samples *A*, *C*, and *E* at low temperature (with preferential in-plane anisotropy) show typical values of B_{hf} close to those for bulk bcc Fe (33.9–3.40 T, Ref. 52), whereas the Tb-covered samples *B*, *D*, and *F* at low temperature (with preferential out-of-

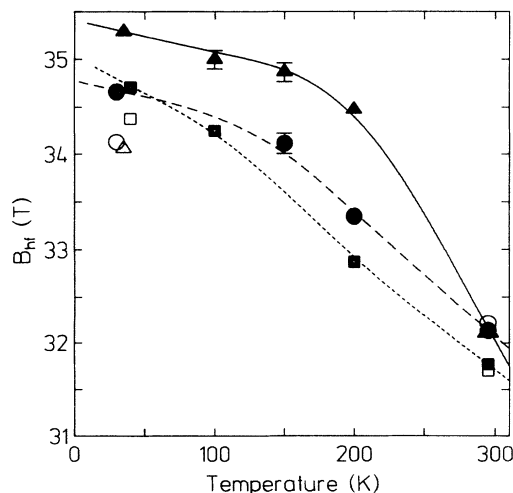


FIG. 9. Measured average hyperfine field B_{hf} as a function of temperature for the different samples studied: sample *A* (open circles); sample *B* (full circles); sample *C* (open triangle); sample *D* (full triangles); sample *E* (open squares); and sample *F* (full squares). (The drawn curves serve as guides to the eyes.)

plane anisotropy) show B_{hf} values which are slightly enhanced in magnitude as compared to those of α -Fe. This effect is most remarkable for sample *D* at 35 K ($B_{\text{hf}} = 35.29$ T), which also shows very strong preferential perpendicular Fe-spin orientation ($\langle \Theta \rangle = 28^\circ$). This weak enhancement in the magnitude of B_{hf} is caused by the local anisotropic demagnetizing field $-N\mu_0 M_s \cos \langle \Theta \rangle$, since the measured hyperfine field B_{hf} (being negative, i.e., opposite to the direction of the spontaneous magnetization M_s) for a single-domain state is given by

$$B_{\text{hf}} = B_{\text{int}} + \frac{1}{3}\mu_0 M_s - N\mu_0 M_s \cos \theta, \quad (1)$$

where B_{int} is the (negative) internal hyperfine field, N is the demagnetizing factor (here $N=1$ for a thin film with M_s oriented perpendicular to the film plane), and Θ is the angle between the direction of M_s and the film normal. The second term in Eq. (1) corresponds to the Lorentz field. The demagnetizing field (third term) is parallel to the (negative) internal hyperfine field and thus enhances the magnitude of B_{hf} for the case of small- Θ values (perpendicular spin texture) as compared to the case of Θ values closer to 90° (in-plane spin texture). By comparing the in-plane (sample *C*) and out-of-plane cases (sample *D*), both at 35 K, and by taking the corresponding values of $\langle \Theta \rangle$ and B_{hf} from Table II, we may estimate the value of $\mu_0 M_s$ for samples *C* and *D* at 35 K from Eq. (1) using $\Theta = \langle \Theta \rangle$. From this we obtain $\mu_0 M_s = (2.0 \pm 0.5)$ T for samples *C* and *D* at 35 K, which is in agreement with the saturation value of 2.19 T for bulk bcc Fe. This demonstrates that the slightly enhanced hyperfine fields in Table II are due to the demagnetizing field and *not* to a transferred hyperfine-field contribution. It also demonstrates that our samples contain predominantly magnetic domains in zero external field with their magnetization aligned along the film-normal direction, since any in-plane domain magnetization present would drastically decrease the demagnetizing field.

IV. DISCUSSION

The influence of the Fe-film thickness on the structure of ultrathin Fe layers deposited on a clean single-crystalline Tb(0001) surface has been shown to be very similar to that found for ultrathin Fe layers on polycrystalline Tb films in Tb/Fe multilayers. At first, for $t_{\text{Fe}} = 3$ and 15 Å, Fe grows on Tb in a noncrystalline, amorphous structure, as demonstrated in Figs. 4(a), 4(b), and 4(c). Above a certain thickness between 15 and 30 Å there is a retrocrystallization of most of the Fe layer [Figs. 4(d) and 4(e)], in good agreement with results for polycrystalline Tb/Fe multilayers^{17,25–28} which show a crystallization thickness in the range 18–32 Å depending on the substrate temperature during film growth.^{17,25} The magnetic properties of our uncoated amorphous Fe films (samples *G* and *H*) have already been discussed in Sec. III.

The magnetic Fe texture of uncovered bcc-Fe layers (30–35 Å thick) on single-crystalline Tb(0001) or on polycrystalline Tb is different from that of such Fe layers in Tb/Fe multilayers: in-plane magnetic Fe texture has been

observed for the uncoated films between ~ 30 and 300 K [Figs. 4(d), 4(e), and 6(a)], while for Tb/Fe multilayers [e.g., with periods of Tb(26 Å)/Fe(30 Å)] below 100 K out-of-plane magnetic Fe texture has been found,^{26–29} implying a stronger total perpendicular magnetic anisotropy for the multilayers as compared to the uncoated single bcc-Fe layers on Tb. Covering the bcc-Fe single layer with 14 Å of Tb, however, leads to a strong tendency for out-of-plane (up to nearly perpendicular) Fe-spin orientation, as is demonstrated in Figs. 5(a)–5(c) and 6(b)–6(d) for samples *B* and *D*, respectively. The results for the uncoated bcc-Fe films [Figs. 4 and 6(a)] indicate that the structure of the Tb substrate (either single crystalline or polycrystalline) plays no determining role for the perpendicular magnetic anisotropy.

The results presented above (and in Fig. 7) for the uncoated Fe- and Tb-covered bcc-Fe layer on Tb(0001) (samples *A* and *B*, respectively) as well as on polycrystalline Tb (samples *C* and *D*, respectively) clearly show the important role of the interface region for creating the perpendicular anisotropy. It is also clear from the above that the two interfaces, Fe deposited onto Tb (i.e., Fe/Tb) and Tb deposited onto Fe (i.e., Tb/Fe), show different properties. Thus we see that for the first samples (samples *A* and *C*), with a Fe/Tb interface only, in-plane Fe-spin texture is observed, while a Tb/Fe interface results in a tendency for out-of-plane Fe-spin texture either for the Tb/Fe/Tb (samples *B* and *D*) or for Tb/Fe/Ag (sample *F*) sandwich structures, with a stronger tendency (smaller $\langle \Theta \rangle$ value) for Tb/Fe/Tb.

The important question is why both types of interfaces (Fe/Tb and Tb/Fe) behave so differently in inducing perpendicular Fe-spin texture (and consequently, perpendicular magnetic anisotropy) in the bcc-Fe layer. We propose that the structure of both types of interfaces may be different. In this context it is important to notice that *in situ* electrical-resistance measurements by Dufour *et al.*¹⁷ on Tb/Fe/Tb triple layers during film deposition have shown an asymmetry in the shape of resistance (or conductance) versus deposited layer thickness. As a possibility, this effect was interpreted in terms of a division of the Fe-layer into an amorphous region near the first (Fe/Tb) interface and a bcc-Fe region which extends from the amorphous zone at the first interface to the second (Tb/Fe) interface.¹⁷ Thus in this interpretation there is a structural asymmetry in both interfaces. Unfortunately, due to the modest counting statistics (i.e., low signal-to-noise ratio) in our CEM spectra of 30–35-Å Fe films [Figs. 4–6 and 8(c)–8(e)], we were not able to detect any weak satellite sextet with broadened lines (in addition to the main bcc-Fe sextet) which may be assigned to an amorphous interface phase.^{17, 18, 25–29} However, based on spectra simulations we cannot exclude that such a weak subspectrum due to a thin amorphous interface exists in our CEM spectra, with an upper limit for its spectral area of $\sim 30\%$ (relative to the total spectral area); this would correspond to an average amorphous Fe-layer thickness of at most ~ 5 Å per interface in our samples, which we cannot exclude. Hence, considering the structural asymmetry reported in Ref. 17 and the present results, we suggest that the Fe-onto-Tb interface (Fe/Tb) (as in uncoat-

ed samples *A*, *C*, and *H*) is much less effective in inducing perpendicular Fe-spin orientation because its structure might be completely amorphous, in contrast to the Tb-onto-Fe interface (Tb/Fe) (as in Tb-coated samples *B* and *D*) which induces a stronger perpendicular Fe-spin orientation at low temperature due to the fact that it might be only partially amorphous (possibly with a different composition or structure than the amorphous phase at the Fe/Tb interface), and contains a large fraction of crystalline bcc Fe, or equivalently, contains a large fraction of regions with a sharp Tb/bcc-Fe interface.

In a recent phenomenological theory, O'Handley and Woods⁵³ have calculated in the zero-field limit the spin structure of α -Fe near a Fe surface showing a strong perpendicular surface anisotropy constant K_S . They find a depth dependence of the Fe-magnetization tilt angle $\Theta(z)$, implying a continuous rotation from the in-plane direction favored in the interior, to perpendicular at the surface. It follows from Figs. 3 and 5 of Ref. 53 that Θ_s (=tilt angle at the surface) and $\langle \Theta \rangle$ (angle Θ averaged over a Fe-surface layer thickness z of 30 or 35 Å, similar to our Fe-film thickness) are proportional to $1/K_S$. For $z=35$ Å, the proportionality constant can be estimated to be about 320 (degrees) $(\text{cm}^2/\text{erg})^{-1}$ from Fig. 3 of Ref. 53. From this and the measured $\langle \Theta \rangle$ values at low temperatures (30–40 K) given in Table II, we can estimate that the effective K_S value is larger for sample *F* (Fe film with one Tb/Fe interface) than for samples *A* or *C* (Fe film with one Fe/Tb interface), consistent with the observation that the Tb/Fe interface is more effective in inducing perpendicular magnetic anisotropy than the Fe/Tb interface. For example, at $T \approx 35$ –40 K the change in $\langle \Theta \rangle$ by $\Delta \langle \theta \rangle = -17^\circ$ for sample *C* relative to sample *F* corresponds to a difference in the reciprocal surface-anisotropy constant, $\Delta(1/K_S)$, of about $-0.05 \text{ cm}^2/\text{erg}$, equivalent to an increase in the relative anisotropy constant, $\Delta K_S/K_S^2$, of about $+0.05 \text{ cm}^2/\text{erg}$ of a Tb/Fe interface as compared to a Fe/Tb interface. Since the boundary conditions in the calculation of Ref. 53 (infinite Fe-film thickness) are different from those of our samples (finite Fe-film thickness) the estimated value for $\Delta(1/K_S)$ (or for $\Delta K_S/K_S^2$) should be considered as a lower (or upper) limit only.

A problem concerns the fact that we still observe a small component of preferential perpendicular Fe-spin orientation according to Fig. 7 even up to room temperature, far above the magnetic ordering temperature of bulk Tb. There is ample evidence that generally in *R/M* multilayers, the *R* atoms at the interface are polarized magnetically by the surrounding magnetic *M* atoms well above the *R* ordering temperature. This has been shown both experimentally^{54–56} and theoretically^{57–59} for Gd/Fe, for Nd/Fe,⁶⁰ and for Tb/Fe.²¹ This phenomenon has also been seen in our Tb/Fe multilayers by observing the magnetic dichroism at the Tb edge⁶¹ at room temperature. Recently, Moschel and Usadel⁶² calculated the magnetic properties of different ferromagnetic layers coupled by antiferromagnetic interactions. They found this effect as well, making this a very general phenomenon. Therefore, PMA observed at room temperature seems to

be related to the polarizing effect of Fe upon Tb at the (sharp) interface.

The temperature dependence of the canting angle $\langle \Theta \rangle(T)$ remains to be explained. Generally, we observe a transition from preferentially perpendicular (small $\langle \Theta \rangle$) to preferentially in-plane Fe-spin texture with increasing temperature (such as in Fig. 7) over a certain range of Fe and Tb thicknesses in multilayers.²⁶⁻²⁹ Wang *et al.*³² made a phenomenological model calculation and ascribed this effect to the magnetic properties of an ultrathin amorphous interface alloy for which they assumed concentration gradients and the same magnetic properties as those in (bulk) amorphous Tb-Fe alloys (sperimagnetic structure) including PMA. Despite the success of this model, the question may be posed whether the continuum model used in these calculations is adequate for the very thin ($\sim 7 \text{ \AA}$) interface phases observed in Fe/Tb multilayers. Recently Jensen and Bennemann⁶³ made a mean-field model calculation of this phenomenon in which the driving force for this transition is the larger entropy due to the increased phase space available for the in-plane configuration. In the later paper⁶⁴ they qualified this conclusion. In their original paper, they used a temperature-independent anisotropy coefficient, inappropriate for a mean-field model. In a very recent quantum-mechanical calculation, Moschel and Usadel⁶⁵ determined the thermally averaged $\langle \Theta \rangle(T)$ for a trilayer assuming a fixed perpendicular surface anisotropy. This new calculation is very interesting because they included the dipolar interaction of the layers (form anisotropy) as well. They found a transition from $\Theta=0^\circ$ at low temperatures to $\Theta=90^\circ$ at higher temperatures, this occurring over a relatively restricted temperature range. Thus we can conclude that the basic driving mechanism for the transition which we observe from perpendicular to in-plane spin texture is the increased entropy due to spin fluctuations.

V. CONCLUSIONS

We have shown Mössbauer-effect (CEMS) results obtained on clean ^{57}Fe films on a well defined Tb(0001) single-crystal or polycrystalline Tb surface. The Fe films exhibit a transition from amorphous to crystalline bcc Fe with increasing Fe thickness between 15 and 30 \AA , in good agreement with results obtained on Tb/Fe (Refs. 16-18 and 24-29) and other R/Fe multilayers.^{19,33,45,48} The Fe-spin texture of thin Fe films on Tb(0001) and on

polycrystalline Tb is in the film plane, contrary to the results obtained for Tb/Fe multilayers which may show perpendicular Fe-spin texture for temperatures less than 100 K.²⁶⁻²⁹ We could show that a perpendicular Fe-spin texture is induced by a Tb/Fe interface obtained by coating the free Fe films with a 14- \AA -thick Tb top layer. This Tb/Fe interface (Tb on Fe) induces a reversible temperature-dependent Fe-spin texture with preferred perpendicular Fe-spin direction at low temperatures and a change to in-plane spin direction for temperatures $\gtrsim 200 \text{ K}$. The results obtained with a polycrystalline Tb substrate are in good agreement with those obtained with the Tb(0001) substrate, leading to the conclusion that the structure of the Tb substrate has no important influence on the magnetic anisotropy in our samples as well as in Tb/Fe multilayers. The importance of the Tb/Fe interface for perpendicular magnetic anisotropy could be confirmed with experiments on Tb/Fe/Ag trilayers. In agreement with Rau and Xing,³⁴ thin Fe films on polycrystalline Ag substrate layers show preferred perpendicular Fe-spin texture after covering with a thin Tb top layer. Comparing the observed changes in average tilting angle $\langle \Theta \rangle$ of Fe spins for a Tb/Fe/Ag trilayer (with one Tb/Fe interface) relative to a Fe film on Tb (with one Fe/Tb interface) with angular changes calculated by O'Handley and Woods⁵³ provides evidence that the magnetic surface anisotropy energy from the Tb/Fe interface is much larger than that from the Fe/Tb interface. Together with results obtained by *in situ* resistance measurements¹⁷ (which indicate a structural asymmetry in both types of interfaces), our present observations suggest that strong perpendicular magnetic anisotropy in UHV-deposited Tb/Fe multilayers originates predominantly at Tb/Fe interfaces which very likely have a different structure than the (less effective) Fe/Tb interfaces. Our results also show that the slightly enhanced hyperfine fields observed in Tb/Fe multilayers with perpendicular Fe-spin texture may be explained by the demagnetizing field, and do not result from transferred hyperfine fields from Tb moments at the interface.

ACKNOWLEDGMENTS

This work could not have been completed without the valuable technical assistance by U. von Hörsten. Work was supported by the Deutsche Forschungsgemeinschaft (SFB 166) and the European Commission (EURAM).

¹P. Chaudhari, J. J. Cuomo, and R. J. Gambino, *Appl. Phys. Lett.* **22**, 337 (1973).

²D. Mergel, H. Heitmann, and P. Hansen, *Phys. Rev. B* **47**, 882 (1993), and references therein.

³T. Morishita, Y. Togami, and K. Tsushima, *J. Phys. Soc. Jpn.* **54**, 37 (1985).

⁴S. Honda, M. Ohkoshi, and T. Kusuda, *IEEE Trans. Magn. MAG-22*, 1221 (1986).

⁵K. Yoden, N. Hosoito, K. Kawaguchi, K. Mibu, and T. Shinjo, *Jpn. J. Appl. Phys.* **27**, 1680 (1988).

⁶N. Sato, *J. Appl. Phys.* **59**, 2514 (1986).

⁷N. Sato and K. Habu, *J. Appl. Phys.* **61**, 4287 (1987).

⁸K. Yamauchi, K. Habu, and N. Sato, *J. Appl. Phys.* **64**, 5748 (1988).

⁹S. Honda, T. Kimura, M. Nawate, and T. Kusuda, *J. Magn. Soc. Jpn.* **15**, 61 (1991).

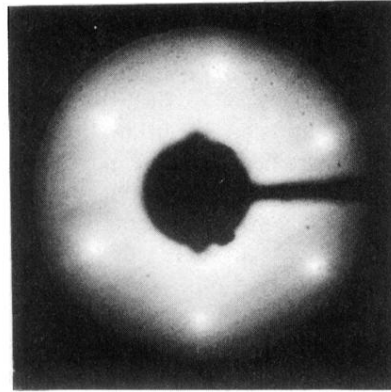
¹⁰S. Honda, T. Kimura, and M. Nawate, *J. Magn. Mater.* **121**, 116 (1993).

¹¹Z. S. Shan, D. J. Sellmyer, S. S. Jaswal, Y. J. Wang, and J. X. Shen, *Phys. Rev. Lett.* **63**, 449 (1989).

¹²Z. S. Shan and D. J. Sellmyer, *Phys. Rev. B* **42**, 10433 (1990).

¹³Z. S. Shan, D. J. Sellmyer, S. S. Jaswal, Y. J. Wang, and J. X.

- Shen, *Phys. Rev. B* **42**, 10446 (1990).
- ¹⁴M. Piecuch, L. T. Baczewski, J. Durand, G. Marchal, P. Delcroix, and H. Nabli, *J. Phys. (Paris) Colloq.* **49**, C8-1755 (1988).
- ¹⁵L. T. Baczewski, M. Piecuch, J. Durand, G. Marchal, and P. Delcroix, *Phys. Rev. B* **40**, 11 237 (1989).
- ¹⁶K. Cherifi, P. Donovan, C. Dufour, Ph. Mangin, and G. Marchal, *Phys. Status Solidi A* **122**, 311 (1990).
- ¹⁷C. Dufour, K. Cherifi, A. Bruson, G. Marchal, and Ph. Mangin, *Phys. Status Solidi A* **125**, 561 (1991).
- ¹⁸K. Cherifi, C. Dufour, M. Piecuch, A. Bruson, Ph. Bauer, G. Marchal, and Ph. Mangin, *J. Magn. Magn. Mater.* **93**, 609 (1991).
- ¹⁹K. Mibu, N. Hosoito, and T. Shinjo, *Hyperfine Interact.* **68**, 341 (1991).
- ²⁰M. Sajieddine, Ph. Bauer, C. Dufour, K. Cherifi, G. Marchal, and Ph. Mangin, *J. Magn. Magn. Mater.* **113**, 243 (1992).
- ²¹C. Dufour, M. Vergnat, K. Cherifi, G. Marchal, Ph. Mangin, and C. Vettier, *Physica B* **180-181**, 489 (1992).
- ²²F. Pierre, P. Boher, R. Kergoat, Ph. Houdy, J. Ferré, and G. Pénissard, *J. Appl. Phys.* **69**, 4565 (1991).
- ²³F. Pierre, P. Boher, Ph. Houdy, J. Ferré, G. Pénissard, V. Grolier, J. Teillet, and A. Fnidiki, *J. Magn. Magn. Mater.* **104-107**, 1033 (1992).
- ²⁴A. Fnidiki, F. Richomme, J. Teillet, F. Pierre, P. Boher, and Ph. Houdy, *J. Magn. Magn. Mater.* **121**, 520 (1993).
- ²⁵J. Teillet, A. Fnidiki, F. Richomme, P. Boher, and Ph. Houdy, *J. Magn. Magn. Mater.* **123**, 359 (1993).
- ²⁶B. Scholz, R. A. Brand, W. Keune, U. Kirschbaum, E. F. Wassermann, K. Mibu, and T. Shinjo, *J. Magn. Magn. Mater.* **93**, 499 (1991).
- ²⁷B. Scholz, R. A. Brand, and W. Keune, *Hyperfine Interact.* **68**, 409 (1991).
- ²⁸B. Scholz, R. A. Brand, and W. Keune, *J. Magn. Magn. Mater.* **104-107**, 1889 (1992).
- ²⁹F. Badia, M. A. Badry, X. X. Zhang, J. Tejada, R. A. Brand, B. Scholz, and W. Keune, *J. Appl. Phys.* **70**, 6206 (1991).
- ³⁰Y. J. Wang and W. Kleeman, *Phys. Rev. B* **44**, 5132 (1991).
- ³¹Y. J. Wang and W. Kleeman, *J. Magn. Magn. Mater.* **115**, 9 (1992).
- ³²Y. J. Wang, C. P. Luo, W. Kleemann, B. Scholz, R. A. Brand, and W. Keune, *J. Appl. Phys.* **73**, 6907 (1993).
- ³³T. Shinjo, *Surf. Sci. Rep.* **12**, 49 (1991).
- ³⁴C. Rau and G. Xing, *J. Vac. Sci. Technol. A* **7**, 1889 (1989).
- ³⁵C. Carbone, R. Rochow, L. Braicovich, R. Jungblut, T. Kachel, D. Tillmann, and E. Kisker, *Phys. Rev. B* **41**, 3866 (1990).
- ³⁶E. Vescovo, R. Rochow, T. Kachel, and C. Carbone, *Phys. Rev. B* **46**, 4788 (1992).
- ³⁷W. Keune, *Hyperfine Interact.* **27**, 111 (1985); W. A. A. Macedo and W. Keune, *Phys. Rev. Lett.* **61**, 475 (1988).
- ³⁸M. Przybylski, J. Korecki, and U. Gradmann, *Appl. Phys. A* **52**, 33 (1991).
- ³⁹N. C. Koon, B. T. Jonker, F. A. Volkening, J. J. Krebs, and G. A. Prinz, *Phys. Rev. Lett.* **59**, 2463 (1987).
- ⁴⁰A. Schatz, S. Dunkhorst, S. Lingnau, U. von Hörsten, and W. Keune, *Surf. Sci.* **310**, L595 (1994).
- ⁴¹W. A. A. Macedo, D. Pelloth, T. Toriyama, O. Nikolov, S. Kruijjer, B. Scholz, R. A. Brand, and W. Keune, *Hyperfine Interact.* (to be published).
- ⁴²W. Kiauka, C. van Cuyck, and W. Keune, *Mater. Sci. Eng. B* **12**, 273 (1992).
- ⁴³S. Ishio, F. Aubertin, T. Limbach, H. Engelmann, I. Dezsi, U. Gonser, S. Fries, M. Takahashi, and M. Fujikura, *J. Phys. F* **18**, 2253 (1988).
- ⁴⁴J. P. Eymery, A. Fnidiki, R. Krishnan, M. Tessier, and J. P. Vitton, *Phys. Rev. B* **38**, 11 931 (1988).
- ⁴⁵S. Handschuh, J. Landes, U. Köbler, Ch. Sauer, G. Kisters, A. Fuss, and W. Zinn, *J. Magn. Magn. Mater.* **119**, 254 (1993).
- ⁴⁶U. Krauss and U. Krey, *J. Magn. Magn. Mater.* **98**, L1 (1991).
- ⁴⁷P. C. M. Gubbens, J. H. F. van Apeldoorn, A. M. van der Kraan, and K. H. J. Buschow, *J. Phys. F* **4**, 921 (1974).
- ⁴⁸T. Shinjo, K. Mibu, S. Ogawa, and N. Hosoito, in *Growth, Characterization and Properties of Ultrathin Magnetic Films and Multilayers*, edited by B. T. Jonker, J. P. Heremans, and E. E. Marinero, MRS Symposia Proceedings No. 151 (Materials Research Society, Pittsburgh, 1990), p. 88.
- ⁴⁹C. J. Gutierrez, M. D. Wiczorek, H. Tang, Z. Q. Qiu, and J. C. Walker, *J. Magn. Magn. Mater.* **99**, 215 (1991).
- ⁵⁰W. Keune, J. Lauer, U. Gonser, and D. L. Williamson, *J. Phys. (Paris) Colloq.* **40**, C2-69 (1979).
- ⁵¹C. J. Gutierrez, S. H. Mayer, Z. Q. Qiu, H. Tang, and J. C. Walker, in *Growth, Characterization and Properties of Ultrathin Magnetic Films and Multilayers* (Ref. 48), p. 17.
- ⁵²R. S. Preston, S. S. Hanna, and J. Heberle, *Phys. Rev.* **128**, 2207 (1962); M. B. Stearns, *ibid.* **162**, 496 (1967).
- ⁵³R. C. O'Handley and J. P. Woods, *Phys. Rev. B* **42**, 6568 (1990).
- ⁵⁴C. Dufour, Ph. Bauer, M. Sajieddine, K. Cherifi, G. Marchal, Ph. Mangin, and R. E. Camley, *J. Magn. Magn. Mater.* **121**, 300 (1992).
- ⁵⁵Ph. Bauer, M. Sajieddine, C. Dufour, K. Cherifi, G. Marchal, and Ph. Mangin, *Europhys. Lett.* **16**, 307 (1991).
- ⁵⁶K. Cherifi, C. Dufour, G. Marchal, Ph. Mangin, and J. Hubsch, *J. Magn. Magn. Mater.* **104-107**, 1833 (1992).
- ⁵⁷R. E. Camley, *Phys. Rev. B* **35**, 3608 (1982).
- ⁵⁸R. E. Camley and D. R. Tilley, *Phys. Rev. B* **37**, 3413 (1988).
- ⁵⁹R. E. Camley, *Phys. Rev. B* **39**, 12 316 (1989).
- ⁶⁰N. Hosoito, K. Mibu, T. Shinjo, and W. Keune, *Hyperfine Interact.* **68**, 337 (1991).
- ⁶¹K. Attenkofer, S. Stähler, M. Knülle, P. Fischer, G. Schütz, G. Wiesinger, and B. Scholz, *J. Appl. Phys.* **73**, 6910 (1993).
- ⁶²A. Moschel and K. Usadel, *J. Magn. Magn. Mater.* (to be published).
- ⁶³P. J. Jensen and K. H. Bennemann, *Phys. Rev. B* **42**, 849 (1990).
- ⁶⁴P. J. Jensen and K. H. Bennemann, *Solid State Commun.* **83**, 1057 (1992).
- ⁶⁵A. Moschel and K. Usadel, *Phys. Rev. B* **49**, 12 868 (1994).



(a)



(b)

FIG. 3. (a) $p(1 \times 1)$ LEED pattern (electron energy 45 eV) and (b) RHEED pattern (electron energy 9 keV) of the clean Tb(0001) surface prior to ^{57}Fe -film deposition.